Article

Not peer-reviewed version

Detection of Sleep Apnea Using Smartphone-Embedded Inertial Measurement Unit

Junichiro Hayano * , Masahiro Takeshima , Aya Imanishi , Masaya Ogasawara , Yasuko Yamada , Emi Yuda , Kazuo Mishima

Posted Date: 18 October 2024

doi: 10.20944/preprints202410.1448.v1

Keywords: acceleration; apnea-hypopnea index; gyroscope; home sleep apnea testing; inertial measurement unit; out-of-center sleep testing; polysomnography; sleep apnea; smartphone; wearable device

 doi:10.20944/preprints202410.1448.v1

Article

Detection of Sleep Apnea Using Smartphone-Embedded Inertial Measurement Unit

Junichiro Hayano [1,*], Masahiro Takeshima [2], Aya Imanishi [2], Masaya Ogasawara [2], Yasuko Yamada [2], Emi Yuda [3] and Kazuo Mishima [2]

[1] Heart Beat Science Lab, Co., Ltd., Sendai 980-8572, Japan
[2] Department of Neuropsychiatry, Akita University Graduate School of Medicine, Akita City 010-8543, Japan
[3] Graduate School of Information Sciences, Tohoku University, Sendai, Japan
* Correspondence: hayano@acm.org; Tel.: +81-80-9725-8259

Abstract: Background: We previously demonstrated that sleep apnea (SA) can be detected using acceleration and gyroscope signals from an inertial measurement unit (IMU) embedded in a wristwatch device. This study aimed to explore whether an IMU embedded in non-wristwatch devices, such as smartphones, can also be used to detect SA, when worn during sleep. Methods: During polysomnography (PSG) examinations, patients wore an IMU-embedded GPS device (Amue Link®) and/or smartphones (Xperia® or iPhone®) on their abdomen. Triaxial acceleration and gyroscope signals from the IMU of each device were recorded overnight. The data were divided into training and test groups in a 2:1 ratio. An algorithm to extract respiratory movements (0.13-0.70 Hz) and detect respiratory events was developed using the training group and its performance was validated in the test group. Results: The estimated respiratory event frequency from the IMU signals of Amue Link, Xperia, and iPhone correlated with the PSG apnea-hypopnea index (AHI), with correlation coefficients of 0.90, 0.93, and 0.96, respectively, in the test group. Using cutoff values derived from the training groups, moderate-to-severe SA (AHI ≥15) was identified with areas under the receiver-operating characteristic curve of 0.95, 0.98, and 0.94, and accuracies of 87%, 94%, and 92%, respectively, in the test groups. Conclusions: SA can be quantitatively detected by IMUs embedded in non-wristwatch devices, including smartphones, when worn during sleep.

Keywords: acceleration; apnea-hypopnea index; gyroscope; home sleep apnea testing; inertial measurement unit; out-of-center sleep testing; polysomnography; sleep apnea; smartphone; wearable device

1. Introduction

Inertial measurement units (IMUs), commonly embedded in wearable devices, have demonstrated potential for continuously capturing acceleration and gyroscope signals with minimal power consumption, making them ideal for long-term sleep monitoring [1–5]. Our previous research showed that an IMU embedded in a wristwatch device can detect apnea-hypopnea respiratory events (REs) in patients with diagnosed or suspected sleep apnea (SA) by capturing subtle linear and rotational arm movements caused by respiration during sleep [6].

This study aims to expand on those findings by investigating whether IMUs embedded in non-wristwatch devices, such as smartphones, can also detect REs. We developed an algorithm to analyze IMU signals from commercially available Android® and iOS® smartphones and a global positioning system (GPS) device worn on the abdomen during sleep. The algorithm's performance in detecting REs was assessed using the apnea-hypopnea index (AHI) from standard polysomnography (PSG) as the reference. The successful implementation of this system across various devices could significantly enhance the accessibility of home-based SA screening, utilizing devices already in widespread use. This could ultimately lead to affordable, low-maintenance solutions for SA detection.

 doi:10.20944/preprints202410.1448.v1

2. Materials and Methods

2.1. Ethics Approval and Consent to Participate

This study was performed according to the protocol that has been approved by Ethics Committee Tohoku University Hospital, Sendai, Japan (registration number 34220, approval date 2023/12/28). All subjects participated in this study gave their written informed consent.

2.2. Subjects

The subjects were patients who underwent overnight PSG from January 2024 to April 2024 at Akita University Hospital (Akita City, Japan) and sleep clinics of Medical Corporation Sound Sleep (Japan) and Medical Corporation Zuimeikai (Japan) for the diagnosis of SA. The inclusion criterion was adults of age between 20 and 80 years who can provide written consent to participate in research of their own free will. Subjects were excluded if they had an acute or chronic illness that required hospitalization within the past 3 months, a history of skin allergies to respiration-sensing bands, etc., were unable to make decisions regarding participation in the study, or were pregnant or possibly pregnant.

2.3. Protocol

Subjects visited the sleep laboratory at the participating facility in the evening and spent overnight in a PSG testing chamber. During the PSG, two IMU devices were attached to the lower abdomen in positions that would not interfere with the polysomnography measurement). The IMU devices were attached using an elastic attachment tool to prevent them from falling off or rotating during measurement (Figure 1).

As the IMU devices, we examined a GPS device (Amue Link® LM-001, Sony Network Communications Inc., Tokyo, Japan), an Android smartphone (Xperia 8® Lite, Sony Corporation, Tokyo, Japan), and an iOS smartphone (iPhone SE® 3rd generation, iOS 17-2-1, Apple Inc., Cupertino, CA, USA). In the following descriptions, the names of these devices will be abbreviated as Amue Link, Xperia, and iPhone, respectively. Two devices, selected at random from Amue Link, Xperia, and iPhone, were attached to each patient.

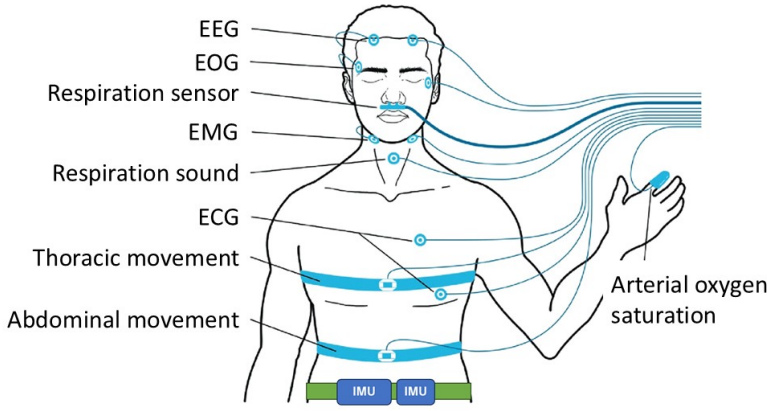

Figure 1. Positions for attaching the sensors for polysomnography and inertial-measurement-unit (IMU)-embedded devices (smartphone and global positioning system device). EEG = electroencephalogram, EOG = electrooculogram, EMG = electromyogram, ECG = electrocardiogram

The PSG recoding was analyzed offline with a sleep diagnostic software (Remlogic version 3.4.1, Natus Medial Incorporated, Middleton, Wisconsin, USA, and DOMINO Ver.3.0.0.6, SOMNO medics, Coral Gables, Florida, USA) and the results of automated analysis were reviewed and edited by expert sleep technicians (Certified Sleep Medicine Examiner by the Japan Sleep Society). The acceleration and gyroscope signals measured by Amue Link were temporarily stored in a buffer and transferred via long-term-evolution-for-machine (LTE-M) communication function for constant network connectivity to a secure cloud storage specifically prepared for this study, while those of

 doi:10.20944/preprints202410.1448.v1

smartphones were stored in memory and transferred to the secure cloud via mobile data communication or Wi-Fi, depending on the sleep laboratory environment.

For each device, patients measured by that device (the patients were partly overlapped between the devices) were randomly divided into training and test groups at a ratio of 2:1, so that only AHI was balanced between the groups. In the training group, an algorithm was developed to detect REs from IMU signals, and a model was created to estimate AHI from RE frequency in IMU signals. In the test group, the performance of the model created in the training group was evaluated.

2.4. Measurement

The PSG was recorded overnight with the standard PSG montages consisting of F4-M1, F3-M2, C4-M1, C3-M2, O2-M1, and O1-M2 electroencephalograms, left and right electrooculograms, a submental electromyogram, a nasal pressure cannula, oronasal airflows, left and right tibial electromyograms, thoracoabdominal inductance plethysmograms, pulse oxy-metric arterial blood oxygen saturation (SpO2), a neck microphone, body position sensors, and a modified lead II ECG.

Respiratory events were scored according to the American Association of Sleep Medicine (AASM) Manual for the Scoring of Sleep and Associated Events, Version 2.5. The average hourly frequencies of apneic episodes, hypopneic episodes, and the combination were defined as apneic index, hypopneic index, and AHI, respectively. The average hourly frequencies of apneic episodes were also measured by the types (obstructive, central, and mixed). Patients with an AHI of 15 or greater 30 were classified as having moderate-to-severe SA.

The acceleration and gyroscope signal of each axis were digitized at a sampling frequency of 32 Hz for Amue Link and 30 Hz for Xperia and iPhone. For all devices, the resolution of acceleration was 0.061 mG per least significant bit (±2.0 G at 16 bit) and that of gyroscope signal was 0.0076 degree per second (dps) per least significant bit (±250 dps at 16 bit).

2.4. Data Analysis

The algorithm developed to detect REs in the IMU signals consisted of the following five steps: extraction of the respiratory component from the acceleration and gyroscope signals, measurement of continuous changes in respiratory amplitude, measurement of continuous changes in respiratory frequency, and detection of REs from respiratory amplitude, and complementary detection of Res from respiratory frequency. In these processes the acceleration signals and gyroscope signals were analyzed in the same way but separately.

2.4.1. Step 1 Extraction of the Respiratory Components

For both acceleration and gyroscope, the X-, Y- and Z-axis signals were processed individually using a band-pass filter (0.13 to 0.70 Hz) to extract the respiratory components of each axis.

2.4.2. Step 2 Measurement of Respiratory Amplitude

The bandpass filtered X-, Y- and Z-axis time series obtained in S1 were combined into a single scalar that reflects the magnitude of respiratory movement as,

$$RA_t = \sqrt{X_t^2 + Y_t^2 + Z_t^2},$$

where RAt represents time series of the magnitude of respiratory movement and Xt, Yt , and Zt indicate band-pass filtered X-, Y-, and Z-axis time series, respectively. RAt was used as an estimate of respiratory amplitude.

2.4.3. Step 3 Measurement of Respiratory Frequency

Of the bandpass filtered X-, Y- and Z-axis time series obtained in S1, the one that most strongly reflected respiratory movement (the one with the largest excursion range) was selected every 30 seconds. The selected time series (length 30 s each) were connected to create a single respiratory wave

 doi:10.20944/preprints202410.1448.v1

time series, adjusting the polarity so that the phase of the junctions matched. After passing through the band-pass filter (0.13 to 0.7 Hz) again, the respiratory cycle lengths were estimated as the interval between the consecutive zero-crossing points from negative to positive in the respiratory wave time series. The time series of respiratory cycle lengths were interpolated using a step function (the instantaneous respiratory cycle length at a given point was assumed to be the respiratory cycle length to which that point belonged), and was converted into a time series of respiratory frequencies (RFt) as the reciprocals sampled at an equal interval.

2.4.4. Step 4 Detection of REs from Respiratory Amplitude

For the time series of estimated respiratory amplitude (RAt) (cyan lines in Figures 2A and 3A), moving averages of the envelope (95th percentile values) with window widths of 3 and 30 seconds were calculated as the fast and slow envelopes, respectively (magenta and blue lines, respectively, in Figures 2A and 3A). Assuming that the fast envelope reflects the breath-by-breath change in the respiratory amplitude and the slow envelope reflects the amplitude flattening the SA-induced change, a >30% reduction in the fast envelope from the slow envelope that continued for 10 to 90 s was detected as an RE (vertical black line with blue triangle in Figure 2A).

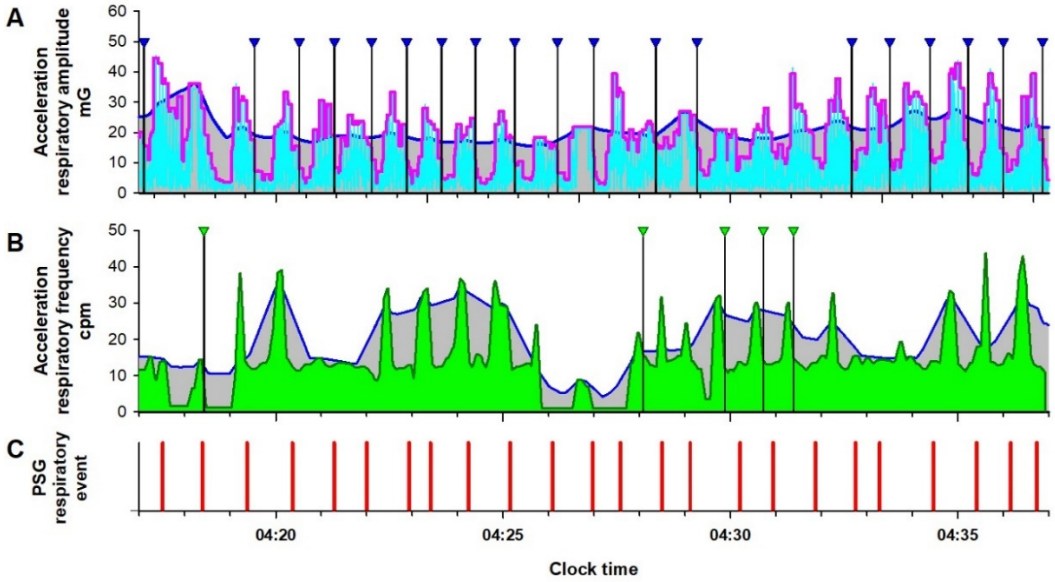

Figure 2. Respiratory amplitude (cyan line in Panel A) and frequency (dark green line in Panel B) extracted from IMU acceleration signal of an Android smartphone in a representative patient with sever sleep apnea during a PSG examination. In Panel A, the magenta and blue lines are the fast and slow envelopes (95th percentiles within 3-s and 30-s moving windows) of the respiratory amplitude, respectively. The black vertical lines with blue triangles are respiratory events (REs) detected as a >30% reduction in the fast envelope from the slow envelope lasting 10 to 90 s. In Panel B, blue line is the upper envelope (95th percentile of 30-s moving window) of the respiratory frequency. Vertical black bars with green triangles are REs detected as >30% reduction in the respiratory frequency from the envelope lasting 10 to 90 s. To avoid double counting of RE by both respiratory amplitude and frequency, the RE detection by the respiratory frequency was suppressed while the fast envelope of the respiratory amplitude was >30% below the slow envelope. In Panel C, vertical red bars are RE (apnea and hypopnea episodes) detected by the simultaneous PSG.

 doi:10.20944/preprints202410.1448.v1

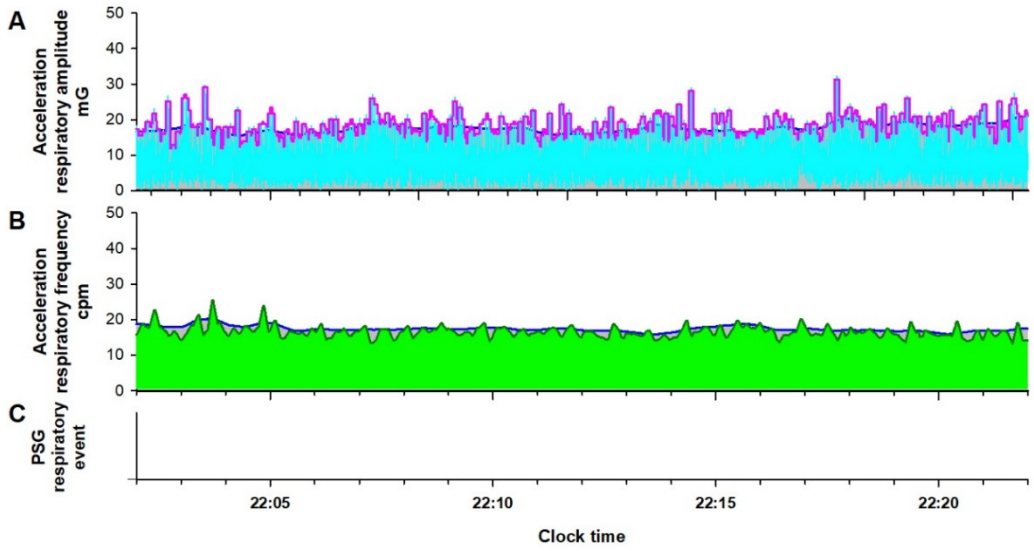

Figure 3. Respiratory amplitude (cyan line in Panel A) and frequency (dark green line in Panel B) extracted from the IMU acceleration signal of an Android smartphone during normal breathing in a patient undergoing a PSG examination. In Panel A, the magenta and blue lines, which show the fast and slow envelopes of the respiratory amplitude, respectively, overlap, and RE is not detected. Panel B, the blue line, which shows the upper envelope of the respiratory frequency, overlaps with the respiratory frequency itself, and RE is also not detected. RE is not detected in the simultaneous PSG (Panel C).

2.4.5. Step 5 Complementary Detection of Res from Respiratory Frequency

For the time series of estimated respiratory frequency (RFt) (dark green lines in Figures 2B and 3B), the upper envelope was calculated as 95th percentile with a window width of 30 s (blue lines in Figures 2B and 3B). Then, a >30% reduction in RFt from the envelope that continued for 10 to 90 s was detected as an RE (vertical black line with green triangle in Figure 2B). To avoid double counting of RE by both RAt and RFt, the RE detection by RFt was suppressed during the fast envelope of RAt was >30% below the slow envelope.

As shown in Figure 3, during normal breathing, the fast and slow envelopes of RAt and the upper envelope of RFt and RFt itself overlap each other, and as the result, RE is not detected. The number of RE detected from RAt and RFt were divided by the monitoring time as respiratory amplitude event index (RAEI) and respiratory frequency event index (RFEI), respectively.

2.5. Creation and Validation of Models to Estimate AHI

In order to verify whether the RAEI and RFEI obtained from the IMU signals can be used to predict SA severity, we created a multiple regression model to calculate the RE index (REI), with PSG AHI as the dependent variable and the RAEI and RFEI of the acceleration and gyroscope signals as the independent variables. The regression model was created using the training group of each device, and the performance of the model was evaluated using the test group. For each device, the optimal cutoff value of the REI to detect patients with moderate-to-severe SA (PSG AHI $\geq$15) was determined using the training group, and the classification performance was evaluated using the test group using the same cutoff value.

2.6. Statistical Analysis

The program package of Statistical Analysis System (SAS institute, Cary, NC, USA) was used for statistical analyses. Differences in quantitative and categorical variables between the training and test groups were evaluated by Wilcoxon rank sum test and $\chi 2$ test. Whereas, differences between

 doi:10.20944/preprints202410.1448.v1

values from acceleration and gyroscope signals in individual subjects were evaluated paired t-test and the relationships were evaluated by the Pearson's correlation coefficient. The multiple regression models to predict PSG AHI by RAEI and RFEI of acceleration signal and those of gyroscope signal were created by the REG procedure, and the model performance was evaluated by the Pearson's correlation coefficient between the PSG AHI and REI (the predicted AHI). The performance of the REI to classify patients with moderate-to-severe SA was evaluated by the area under the curve (AUC) of the receiver-operating characteristic (ROC) curve. The optimal cutoff value of the REI for classification determined in the training group was examined in the test group with the sensitivity, specificity, accuracy, and positive and negative predictive values (PPV and NPV, respectively). Statistical significance was considered for $P < 0.05$.

3. Results

3.1. Subjects' Characteristis

Data for Amue Link, Xperia, and iPhone were obtained in 46, 46, and 36 patients, respectively. They had median ages (IQR) of 44 (33-56), 48 (42 to 62), and 45 (33 to 53), median body mass indices (IQR) of 26.3 (23.2 to 30.4), 26.6 (23.3 to 30.4), and 24.4 (21.2 to 27.2) kg/m2, and median PSG AHIs (IQR) of 14.2 (5.9 to 31.3), 19.3 (7.7 to 38.7), and 12.1 (5.5 to 32.9), respectively.

The subjects measured by each device were divided into the training group and the test group. For all devices, there was no significant difference in subjects' characteristics between the two groups (Table 1).

Table 1. Subjects' characteristics in training and test groups for each device.

	Amue Link		Xperia		iPhone	
	Training group *n* = 31	**Test group *n* = 15**	**Training group *n* = 30**	**Test group *n* = 16**	**Training group *n* = 22**	**Test group *n* = 12**
Age, year	42 (31-53)	53 (40-61)	48 (39-60)	53 (43-64)	44 (32-52)	47 (36-54)
Female, *n* (%)	3 (19%)	3 (10%)	3 (10%)	1 (6%)	6 (25%)	3 (25%)
BMI, kg/m2	26.7 (23.4-30.4)	24.3 (21.6-30.7)	26.2 (22.5-28.7)	27.4 (23.8-31.9)	24.1 (21.6-27.1)	24.9 (20.9-27.3)
Polysomnography						
TRT, min	465 (388-497)	472 (414-477)	531 (496-554)	516 (491-553)	512 (482-545)	534 (486-565)
TST, min	404 (354-435)	403 (298-445)	393 (346-431)	406 (353-424)	384 (313-438)	394 (303-445)
Sleep efficiency, %	81.3 (71.5-86.2)	83.9 (75.5-93.5)	91.9 (78.1-87.7)	80.9 (70.5-89.2)	85.2 (79.4-91.1)	85.6 (77.3-91.9)
Sleep latency, min	7.0 (0.0-18.5)	5.0 (0.0-11.5)	32.3 (15.0-55.0)	23.3 (12.5-67.0)	23.0 (10.5-57.0)	29.8 (11.8-49.8)
WASO, min	28.5 (19.0-44.0)	28.5 (16.3-43.3)	43.0 (30.5-95.8)	40.8 (30.5-57.3)	37.3 (26.5-56.5)	30.5 (20.3-64.3)
Sleep stage						
N1, %	21 (14-31)	30 (14-35)	21 (13-34)	31 (18-41)	20 (12-32)	26 (15-32)
N2, %	50 (38-60)	49 (42-52)	49 (33-54)	49 (41-59)	53 (43-62)	50 (42-53)
N3, %	12 (6-21)	11 (3-21)	11 (5-23)	4 (2-7)	15 (8-22)	5 (2-18)
REM, %	9 (3-16)	9 (3-19)	12 (7-19)	8 (4-20)	4 (1-16)	18 (4-23)
AHI	15.8 (8.6-37.4)	15.4 (8.5-36.7)	24.0 (10.4-45.0)	24.4 (9.5-46.7)	12.0 (5.4-30.2)	14.7 (6.7-34.7)
OAI	3.5 (0.9-8.1)	4.5 (1.3-7.2)	7.4 (1.2-18.1)	5.5 (0.93-13.8)	3.9 (0.7-5.7)	2.7 (1.0-7.0)
CAI	0.4 (0.2-1.9)	0.6 (0.2-2.8)	0.7 (0.1-2.0)	2.1 (0.2-4.1)	0.5 (0.2-0.9)	0.8 (0.4-2.5)
MAI	0.3 (0.1-1.8)	0.2 (0.0-0.8)	0.4 (0.2-1.8)	0.9 (0.1-3.2)	0.2 (0.0-1.0)	0.5 (0.3-1.3)
HI	12.4 (4.3-19.4)	8.3 (2.1-15.2)	10.5 (7.4-19.9)	18.0 (4.4-22.8)	9.4 (3.5-15.1)	7.5 (3.9-15.2)
AHI ≥15	16 (52%)	8 (53%)	20 (67%)	11 (69%)	10 (45%)	6 (50%)
AHI ≥30	10 (32%)	5 (33%)	12 (40%)	6 (38%)	6 (27%)	3 (25%)

 doi:10.20944/preprints202410.1448.v1

Data are median (IQR) or frequency (%). For all devices, there is no significant difference between the training and test groups for any of the parameters. AHI = apnea-hypopnea index, BMI = body mass index, CAI = central apnea index, HI = hypopnea index, MAI = mixed apnea index, OAI = obstructive apnea index, TRT = total recording time, TST = total sleep time, WASO = wake after sleep onset.

3.2. Development of Algorithms and Models to Estimate AHI from IMU Signals in the Training Groups

Analysis of data from the Amue Link, Xperia, and iPhone training groups revealed that the algorithm described in the Data Analysis section could be applied to both the acceleration and gyroscope signals of all three devices to detect RE and calculate RAEI and RFEI. Although the RAEI measured from the acceleration signal was smaller than that from the gyroscope signal, the two were closely correlated across all three devices (Table 2). Conversely, there was no significant difference between the RFEIs measured from the acceleration and gyroscope signals across devices, although the level of correlation varied among them. Furthermore, the relationships between RAEI and RFEI from IMU signals and the PSG AHI differed between the three devices. Therefore, multiple regression models to estimate PSG AHI from these indices were developed separately for each device, using the RAEI and RFEI from both acceleration and gyroscope signals in their respective training groups.

Table 2. Comparison of hourly frequencies of respiratory events (RE) observed in the respiratory amplitude and respiratory frequency between the acceleration and gyroscope signals in the training group of each device.

	RAEI				**RFEI**			
	Acceleration	**Gyroscope**	***P****	***r***	**Acceleration**	**Gyroscope**	***P****	***r***
Amue Link	10.9 ± 8.3	12.5 ± 10.4	0.03	0.93	11.3 ± 8.7	12.5 ± 8.6	0.3	0.65
Xperia	13.9 ± 11.0	18.0 ± 13.9	<0.0001	0.98	11.3 ± 8.3	11.1 ± 7.8	0.6	0.90
iPhone	11.6 ± 9.5	14.8 ± 13.0	0.002	0.98	11.2 ± 7.6	11.6 ± 6.2	0.6	0.85

RAEI = hourly frequency of respiratory event detected from respiratory amplitude, RFEI = hourly frequency of respiratory event detected from respiratory frequency, r = correlation coefficient between values from acceleration and gyroscope signals. *Significance of difference of paired t-test between values from acceleration and gyroscope signals.

Table 3 shows the multiple regression coefficients of the RAEI and RFEI for predicting the PSG AHI in the training group of each device. The relationships between PSG AHI and the REI calculated by the regression models in the training groups are presented in Panels A-C in Figure 4. For all devices, the REI showed a good correlation with PSG AHI (r = 0.96, 0.94, and 0.84 for Amue Link, Xperia, and iPhone, respectively).

Table 3. AHI regression model coefficients of hourly frequencies of respiratory events (RE) obtained from the respiratory amplitude and frequency of the acceleration and gyroscope signals in the training group of each device.

	Regression coefficient				
	Acceleration		**Gyroscope**		**Intercept**
	RAEI	**RFEI**	**RAEI**	**RFEI**	
Amue Link	1.71	0.20	0.82	-0.44	-2.60
Xperia	1.43	0.17	0.84	0.21	-5.64
iPhone	0.34	0.95	0.71	-0.62	1.36

Abbreviations are defined in the footnote to Table 2.

 doi:10.20944/preprints202410.1448.v1

In the training group, the REIs obtained from the models for Amue Link, Xperia, and iPhone discriminated subjects with moderate to severe SA (AHI ≥ 15) with ROC analysis AUCs of 0.92, 0.97, and 0.94 and classification accuracies of 84%, 93%, and 82%, respectively (Table 4).

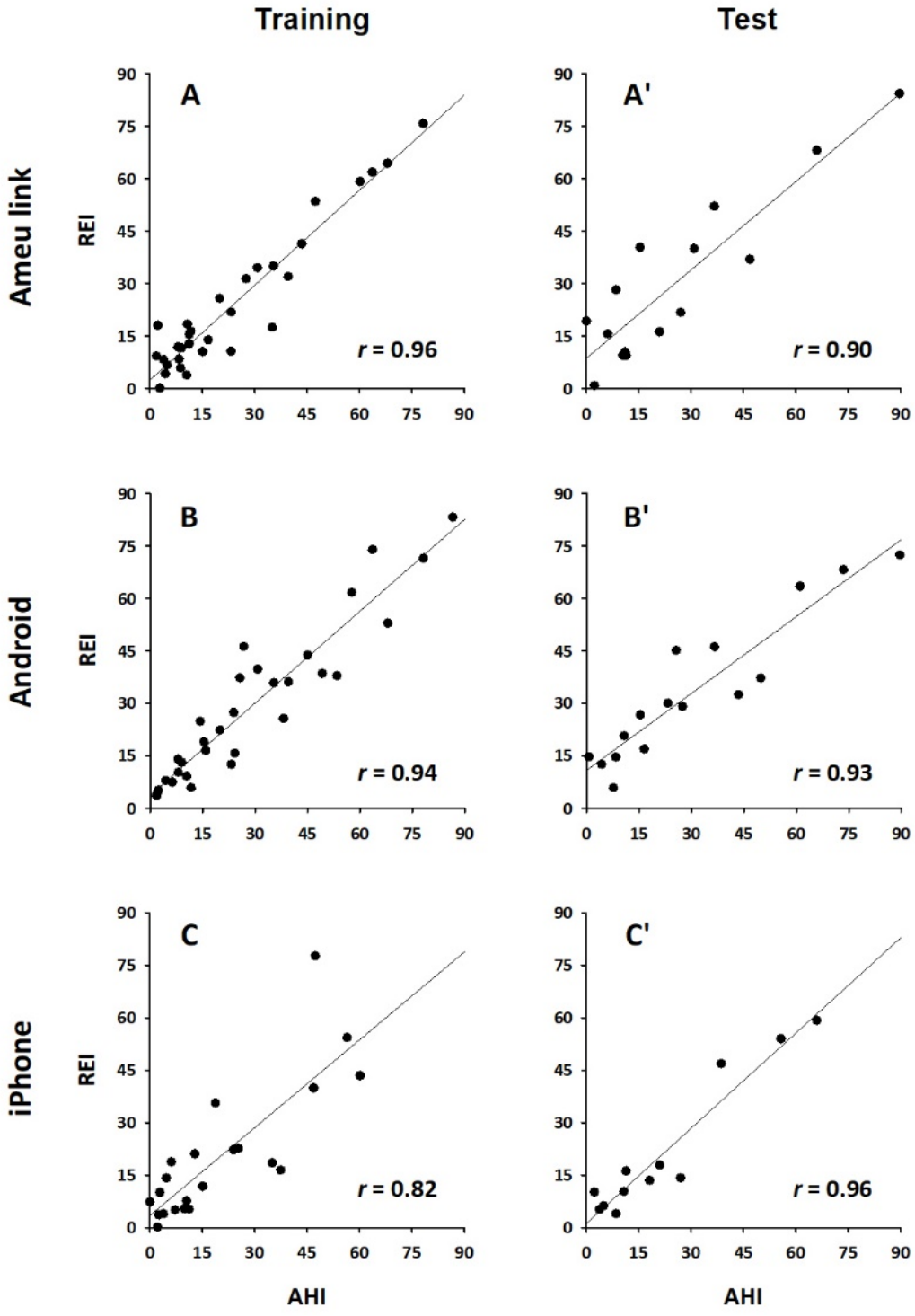

Figure 4. Relationships between apnea-hypopnea index (AHI) of polysomnography and respiration event index (REI) obtained from IMU signals in the training (A-C) and test groups (A′-C′) of each device; A and A′: Amue Link, B and B′: Xperia, and C and C′: iPhone. r = correlation coefficient.

 doi:10.20944/preprints202410.1448.v1

Table 4. Classification performance of each device for moderate to severe sleep apnea (AHI ≥ 15) by REI in the training and test groups.

Device	Group	AUC (SE)	REI cutoff*	Sensitivity	Specificity	PPA	NPA	Accuracy
Amue Link	Training	0.92 (0.049)	≥16	81%	87%	87%	81%	84%
	Test	0.95 (0.053)		100%	72%	80%	100%	87%
Xperia	Training	0.97 (0.030)	≥15	95%	90%	95%	90%	93%
	Test	0.98 (0.026)		100%	80%	92%	100%	94%
iPhone	Training	0.94 (0.045)	≥13	90%	75%	75%	90%	82%
	Test	0.94 (0.066)		100%	83%	86%	100%	92%

* Cutoff values for REI were determined for each device in the training group and applied to the test group for that device. NPA = negative predictive accuracy and PPA = positive predictive accuracy.

3.3. Validation of Models in the Test Groups

The multiple regression model created for estimating PSG AHI in the training group of each device was applied to the test group of each device. The relationships between PSG AHI and the estimated REI by the regression models in the test groups are presented in Panels A′-C′ in Figure 4. For all devices, the REI estimated by the model showed a good correlation with PSG AHI (r = 0.90, 0.93, and 0.96 for Amue Link, Xperia, and iPhone, respectively). In the test groups, the REIs obtained from the models for Amue Link, Xperia, and iPhone discriminated subjects with moderate to severe SA with ROC analysis AUCs of 0.95, 0.98, and 0.94, respectively (Table 4).

For all devices, the correlation coefficients with AHI and the AUCs of classification performance in the test group were not substantially lower than those in the training group (Figure 4 and Table 4), suggesting that the obtained models were not over-fitted to the training group. When the cut-off values determined for Amue Link, Xperia and iPhone in the training groups were applied to the REIs obtained from the models for the individual devices, the moderate to severe SA patients in the test groups were classified with 87%, 94% and 92% accuracy, respectively (Table 4).

4. Discussion

The present study demonstrated that SA can be quantitatively detected using only IMUs embedded in non-wristwatch devices, including smartphones. Combined with our previous finding that SA can be detected by an IMU embedded in a wristwatch device [6], these results suggest that almost all wearable devices can be effectively used for quantitative SA screening, as long as they are equipped with an IMU. Since many wearable devices already have a built-in IMU, our findings have the potential to greatly improve the accessibility of SA screening at home by utilizing devices that are already widely available. Furthermore, this could lead to the development of new, inexpensive, easy-to-use devices designed as SA detectors, capable of long-term operation without recharging.

Many smartphone applications aim to encourage timely medical care for SA. Although many lack diagnostic accuracy, and their algorithms are often proprietary and unverifiable [7,8], some models using smartphone-recorded breathing sounds have shown potential for predicting obstructive SA [9–11]. For example, Cho et al. [9] used a smartphone placed 1 m from the patient's head during PSG to record breathing sounds, extracting 508 features for machine learning. Their random forest model detected moderate-to-severe SA with an AUC of 0.89, sensitivity of 87.3%, specificity of 70.6%, and accuracy of 82.3%. Similarly, Le et al. [10] used a smartphone 1 m away from the patient, applying a neural network model to classify 30-second epochs as "no event," "apnea," or "hypopnea" based on spectral features of sound energy. Their model's REI correlated with PSG AHI (r = 0.98) and identified moderate-to-severe SA with an AUC of 0.85, sensitivity of 85%, and specificity of 84%. The IMU signal-based classification performance in the present study was comparable to those of sound-based methods but has potential advantages, including a more straightforward

 doi:10.20944/preprints202410.1448.v1

physiological algorithm, the ability to detect all types of SA, including central SA, and broader applicability to other widely used wearable devices.

Two points need to be mentioned about the methods of the present study. First, we detected respiratory movement using an IMU attached to the abdomen. The respiratory amplitude measured by the abdominal IMU (acceleration 10-30 mG and gyroscope 10-30 dps) was approximately 10 times greater than that recorded by a wristwatch IMU in our previous study (1-3 mG and 1-3 dps, respectively) [6], indicating a higher signal-to-noise ratio. However, this increased sensitivity also made it easier to detect respiratory effort during obstructive apnea, making the reduction in respiratory amplitude less apparent and occasionally leading to missed detections of obstructive apnea (Panel A, Figure 2). To address this, we introduced an auxiliary detection method based on the contrast between respiratory frequency during apnea and that during resumption of breathing (Panel B, Figure 2). Since respiratory frequency does not always decrease even when respiratory amplitude drops during apnea, these two methods complement each other effectively.

Second, we analyzed the acceleration and gyroscope signals in parallel and calculated the RAEI and RFEI from each signal. Although the RAEI detected from the acceleration signal was lower than that from the gyroscope, the two were closely correlated. The RFEI values from the acceleration and gyroscope signals were similar, though the level of correlation varied among devices. These findings suggest that respiration induces both linear and rotational movements of the abdomen, and that SA leads to transient reductions in their amplitude and frequency in a device-dependent manner. Therefore, we developed models to predict the REI using both the RAEI and RFEI from the acceleration and gyroscope signals for each individual device.

SA is a common but underdiagnosed condition that significantly increases the risk of lifestyle-related diseases such as hypertension, diabetes, cardiovascular disease, and dementia [12–14]. It is also a direct cause of sleep-related accidents and reduced productivity, often referred to as presenteeism [14,15]. Despite its serious health implications, over 80% of SA patients remain undiagnosed and untreated [16], creating a substantial burden on healthcare systems [17,18]. One of the main reasons for this low diagnosis rate is the limited availability of medical facilities capable of conducting PSG, the gold standard for SA diagnosis [19]. Many patients do not seek medical attention unless they experience severe symptoms, and even simple screening devices for sleep apnea are not widely accessible [20].

In this context, our finding that IMU signals can be used for quantitative SA screening could greatly enhance the accessibility of SA screening at home, leveraging the widespread availability of IMU-embedded wearable devices. Furthermore, the SA detection capability of the IMU may lead to the development of inexpensive, easy-to-use devices for integrating the Internet of Things (IoT) aimed at improving sleep quality. For example, positional sleep apnea (AHI in the supine position ≥ 2 × AHI in other positions) has been reported in 55 to 61% of patients with obstructive SA [21,22], and the effectiveness of positional therapies, such as cervical vertebrae support with head tilting and scapula support in the lateral position [23], as well as head-of-bed elevation [24–26], has also been demonstrated. Continuous SA monitoring with IMU devices linked to IoT-enabled pillows and beds could enable AI-driven feedback therapeutic systems, offering real-time adjustments for optimal sleep positioning.

This study has limitations. The algorithm and models were developed using data from patients with suspected SA (pretest probability 45-67%) during PSG examinations. If these results are applied to the general population, where the pretest probability of SA is lower, or to data collected in a home environment, the sensitivity and positive predictive accuracy may not be as high.

5. Conclusions

Acceleration and gyroscope signals from an IMU embedded in a non-wristwatch device can be used to detect SA episodes and estimate SA severity in adults with suspected SA. Combined with our previous findings on quantitative SA detection using a wristwatch IMU, this approach has the potential to significantly enhance the accessibility of home-based SA screening by leveraging widely available IMU-embedded devices.

Author Contributions: Conceptualization, J.H., E.Y. and K.M.; methodology, J.H.; software, J.H.; validation, E.Y. and K.M.; formal analysis, E.Y.; investigation, J.H.; resources, K.M.; data curation, M.T., A.I., M.O., and Y.Y.; writing—original draft preparation, J.H.; writing—review and editing, E.Y. and K.M.; visualization, J.H.; project administration, K.M.; funding acquisition, J.H. and K.M. All authors have read and agreed to the published version of the manuscript.

Funding: This research was funded by Sony Group Corporation, Tokyo, Japan.

Institutional Review Board Statement: This study was performed according to the protocol that has been approved by Ethics Committee Tohoku University Hospital, Sendai, Japan (registration number 34220, approval date 2023/12/28).

Informed Consent Statement: Informed consent was obtained from all subjects involved in the study. request.

Data Availability Statement: The datasets generated during and/or analyzed during the current study are available from the corresponding author on reasonable request.

Conflicts of Interest: J.H. is the President and E.Y. is the Chief Technical Officer of Heart Beat Science Lab Inc., which received funding for this study from Sony Group Corporation. K.M. is a professor of Akita University Graduate School of Medicine., which received funding for this study from Sony Group Corporation. The other authors declare no competing interests. The funders had no role in the design of the study; in the collection, analyses, or interpretation of data; in the writing of the manuscript; or in the decision to publish the results.

References

1. Buckley, N.; Davey, P.; Jensen, L.; Baptist, K.; Jansen, B.; Campbell, A.; Downs, J., Can Wearable Inertial Measurement Units Be Used to Measure Sleep Biomechanics? Establishing Initial Feasibility and Validity. *Biomimetics (Basel)* **2022**, *8*, (1).
2. McDevitt, B.; Moore, L.; Akhtar, N.; Connolly, J.; Doherty, R.; Scott, W., Validity of a Novel Research-Grade Physical Activity and Sleep Monitor for Continuous Remote Patient Monitoring. *Sensors* **2021**, *21*, (6).
3. Bansal, K.; Garcia, J.; Feltch, C.; Earley, C.; Robucci, R.; Banerjee, N.; Brooks, J., A pilot study to understand the relationship between cortical arousals and leg movements during sleep. *Scientific reports* **2022**, *12*, (1), 12685.
4. Taebi, A.; Solar, B. E.; Bomar, A. J.; Sandler, R. H.; Mansy, H. A., Recent Advances in Seismocardiography. *Vibration* **2019**, *2*, (1), 64-86.
5. Ode, K. L.; Shi, S.; Katori, M.; Mitsui, K.; Takanashi, S.; Oguchi, R.; Aoki, D.; Ueda, H. R., A jerk-based algorithm ACCEL for the accurate classification of sleep-wake states from arm acceleration. *iScience* **2022**, *25*, (2), 103727.
6. Hayano, J.; Adachi, M.; Sasaki, F.; Yuda, E., Quantitative detection of sleep apnea in adults using inertial measurement unit embedded in wristwatch wearable devices. *Scientific reports* **2024**, *14*, (1), 4050.
7. Kapur, V. K.; Auckley, D. H.; Chowdhuri, S.; Kuhlmann, D. C.; Mehra, R.; Ramar, K.; Harrod, C. G., Clinical Practice Guideline for Diagnostic Testing for Adult Obstructive Sleep Apnea: An American Academy of Sleep Medicine Clinical Practice Guideline. *J Clin Sleep Med* **2017**, *13*, (3), 479-504.
8. Baptista, P. M.; Martin, F.; Ross, H.; O'Connor Reina, C.; Plaza, G.; Casale, M., A systematic review of smartphone applications and devices for obstructive sleep apnea. *Braz J Otorhinolaryngol* **2022**, *88* Suppl 5, (Suppl 5), S188-s197.
9. Cho, S. W.; Jung, S. J.; Shin, J. H.; Won, T. B.; Rhee, C. S.; Kim, J. W., Evaluating Prediction Models of Sleep Apnea From Smartphone-Recorded Sleep Breathing Sounds. *JAMA Otolaryngol Head Neck Surg* **2022**, *148*, (6), 515-521.
10. Le, V. L.; Kim, D.; Cho, E.; Jang, H.; Reyes, R. D.; Kim, H.; Lee, D.; Yoon, I. Y.; Hong, J.; Kim, J. W., Real-Time Detection of Sleep Apnea Based on Breathing Sounds and Prediction Reinforcement Using Home Noises: Algorithm Development and Validation. *J Med Internet Res* **2023**, *25*, e44818.
11. Han, S. C.; Kim, D.; Rhee, C. S.; Cho, S. W.; Le, V. L.; Cho, E. S.; Kim, H.; Yoon, I. Y.; Jang, H.; Hong, J.; Lee, D.; Kim, J. W., In-Home Smartphone-Based Prediction of Obstructive Sleep Apnea in Conjunction With Level 2 Home Polysomnography. *JAMA Otolaryngol Head Neck Surg* **2024**, *150*, (1), 22-29.
12. Somers, V. K.; White, D. P.; Amin, R.; Abraham, W. T.; Costa, F.; Culebras, A.; Daniels, S.; Floras, J. S.; Hunt, C. E.; Olson, L. J.; Pickering, T. G.; Russell, R.; Woo, M.; Young, T., Sleep apnea and cardiovascular disease: an American Heart Association/American College Of Cardiology Foundation Scientific Statement from the American Heart Association Council for High Blood Pressure Research Professional Education Committee, Council on Clinical Cardiology, Stroke Council, and Council On Cardiovascular Nursing. In collaboration with the National Heart, Lung, and Blood Institute National Center on Sleep Disorders Research (National Institutes of Health). *Circulation* **2008**, *118*, (10), 1080-111.
13. Gharibeh, T.; Mehra, R., Obstructive sleep apnea syndrome: natural history, diagnosis, and emerging treatment options. *Nature and science of sleep* **2010**, *2*, 233-55.

 doi:10.20944/preprints202410.1448.v1

14. Morsy, N. E.; Farrag, N. S.; Zaki, N. F. W.; Badawy, A. Y.; Abdelhafez, S. A.; El-Gilany, A. H.; El Shafey, M. M.; Pandi-Perumal, S. R.; Spence, D. W.; BaHammam, A. S., Obstructive sleep apnea: personal, societal, public health, and legal implications. *Rev. Environ. Health* **2019**, *34*, (2), 153-169.
15. Léger, D.; Stepnowsky, C., The economic and societal burden of excessive daytime sleepiness in patients with obstructive sleep apnea. *Sleep medicine reviews* **2020**, *51*, 101275.
16. Peppard, P. E.; Young, T.; Barnet, J. H.; Palta, M.; Hagen, E. W.; Hla, K. M., Increased prevalence of sleep-disordered breathing in adults. *Am. J. Epidemiol.* **2013**, *177*, (9), 1006-14.
17. Benjafield, A. V.; Ayas, N. T.; Eastwood, P. R.; Heinzer, R.; Ip, M. S. M.; Morrell, M. J.; Nunez, C. M.; Patel, S. R.; Penzel, T.; Pépin, J. L.; Peppard, P. E.; Sinha, S.; Tufik, S.; Valentine, K.; Malhotra, A., Estimation of the global prevalence and burden of obstructive sleep apnoea: a literature-based analysis. *Lancet Respir Med* **2019**, *7*, (8), 687-698.
18. Faria, A.; Allen, A. H.; Fox, N.; Ayas, N.; Laher, I., The public health burden of obstructive sleep apnea. *Sleep Sci* **2021**, *14*, (3), 257-265.
19. Epstein, L. J.; Kristo, D.; Strollo, P. J., Jr.; Friedman, N.; Malhotra, A.; Patil, S. P.; Ramar, K.; Rogers, R.; Schwab, R. J.; Weaver, E. M.; Weinstein, M. D., Clinical guideline for the evaluation, management and long-term care of obstructive sleep apnea in adults. *J Clin Sleep Med* **2009**, *5*, (3), 263-76.
20. Punjabi, N. M., The epidemiology of adult obstructive sleep apnea. *Proc Am Thorac Soc* **2008**, *5*, (2), 136-43.
21. Richard, W.; Kox, D.; den Herder, C.; Laman, M.; van Tinteren, H.; de Vries, N., The role of sleep position in obstructive sleep apnea syndrome. *Eur. Arch. Otorhinolaryngol.* **2006**, *263*, (10), 946-50.
22. Garg, H.; Er, X. Y.; Howarth, T.; Heraganahally, S. S., Positional Sleep Apnea Among Regional and Remote Australian Population and Simulated Positional Treatment Effects. *Nature and science of sleep* **2020**, *12*, 1123-1135.
23. Lee, J. B.; Park, Y. H.; Hong, J. H.; Lee, S. H.; Jung, K. H.; Kim, J. H.; Yi, H.; Shin, C., Determining optimal sleep position in patients with positional sleep-disordered breathing using response surface analysis. *J. Sleep Res.* **2009**, *18*, (1), 26-35.
24. Souza, F.; Genta, P. R.; de Souza Filho, A. J.; Wellman, A.; Lorenzi-Filho, G., The influence of head-of-bed elevation in patients with obstructive sleep apnea. *Sleep Breath* **2017**, *21*, (4), 815-820.
25. Iannella, G.; Cammaroto, G.; Meccariello, G.; Cannavicci, A.; Gobbi, R.; Lechien, J. R.; Calvo-Henríquez, C.; Bahgat, A.; Di Prinzio, G.; Cerritelli, L.; Maniaci, A.; Cocuzza, S.; Polimeni, A.; Magliulo, G.; Greco, A.; de Vincentiis, M.; Ralli, M.; Pace, A.; Polimeni, R.; Lo Re, F.; Morciano, L.; Moffa, A.; Casale, M.; Vicini, C., Head-Of-Bed Elevation (HOBE) for Improving Positional Obstructive Sleep Apnea (POSA): An Experimental Study. *Journal of clinical medicine* **2022**, *11*, (19).
26. Lee, S.; Park, J. H.; Kim, J. Y.; Park, S. W.; Shin, H. B.; Kim, B. H., Implementation of Head of Bed Elevation Using Adjustable Bed and Its Effects on Sleep: A Pilot Randomized Trial. *Altern. Ther. Health Med.* **2024**.